Preparation and Characterization of PVA/OMMT Composites

Caner Yürüdü,[1] Sevim İşçi,[1] Cüneyt Ünlü,[2] Oya Atıcı,[2] Ö. Işık Ece,[3] Nurfer Güngör[1]

[1] *İ.T.Ü., Department of Physics, Faculty of Science and Letters, Maslak 34469, Istanbul, Turkey*
[2] *İ.T.Ü., Department of Chemistry, Faculty of Science and Letters, Maslak 34469, Istanbul, Turkey*
[3] *İ.T.Ü., Department of Geology, Faculty of Mines, Maslak 34469, Istanbul, Turkey*

Received 8 December 2005; accepted 10 March 2006
DOI 10.1002/app.24452
Published online in Wiley InterScience (www.interscience.wiley.com).

ABSTRACT: In this study, polyvinyl alcohol/organically modified montmorillonite (HDA/MMT; organoclay) composite was prepared for the intercalation processes. Firstly, the rheological behavior of aqueous montmorillonite dispersions was investigated as a function of solid content. Hexadecylamine (HDA) was added to the montmorillonite dispersion (2%, w/w) in different concentrations in the range of $5 \times 10^{-4} - 9 \times 10^{-3}$ mmol/L. The basal spacing of the organoclay (OMMT) was studied by X-ray diffraction. The FTIR spectra are obtained from the modified montmorillonite products, which revealed the characteristic absorbencies after treatment with HDA. HDA/MMT /PVA composite, which was produced by the reaction of 1 wt % PVA solution with organoclay complex, is characterized by the rheology, electrokinetic, XRD, FTIR, and SEM techniques. © 2006 Wiley Periodicals, Inc. J Appl Polym Sci 102: 2315–2323, 2006

Key words: montmorillonite; hexadecylamine; organoclay; composite; rheology; ζ potential

INTRODUCTION

Layered smectite-type montmorillonite is a hydrous alumina silicate mineral whose lamellae are constructed from octahedral alumina sheets sandwiched between two tetrahedral silicate sheets, exhibits a net negative charge on the lamellar surface, which enables them to adsorb cations, such as Na^+ or Ca^+. Montmorillonite dispersions are sensitive to the exchangeable cations and pH. The valency of the exchangeable cations, monovalent or divalent, has a strong influence on the flow properties.[1–3] Montmorillonite minerals are commonly used in various industrial products and processes. The determination of the rheological characteristics, such as viscosity and thixotropy, which are known to possess great importance in the clay–water suspensions, are important for many industry, such as the ceramic, sanitary, drilling, paper, and detergent industries.

Surface properties of natural clays can be modified by simple ion exchange with organic cations. Clays are easily modified by exchanging their inorganic cations with quaternary ammonium cations.[4–7] Montmorillonite belongs to 2 : 1 group of dioctahedral smectite group and its swelling properties changes depending on its structure of ions holding between the layers of unit cells. These ions exchange properties not only provide the diffusion of large molecule components into the layers of montmorillonite minerals and also can enable to exchange large molecules components with available cation between the layers. As the organic cations are replaced by the organic cations, the surface properties of clay may change considerably from highly hydrophilic to increasingly organophilic.

Organic and inorganic materials affect the rheological properties of montmorillonite dispersions when they interact with the clay minerals. Organoclays are produced by an ion exchange reaction, where organic materials replace with the exchangeable cations on a montmorillonite surface. During this reaction, the clay changes from hydrophilic to organophilic and is converted to an organoclay.[7–9] Nowadays, industrial applications of composites are exponentially increasing. Recently, nanoscale composites of polymers with organoclay have been studied extensively. Montmorillonite is the most widely used layered silicate in polymer nanocomposites.[10–17] The main purpose of researchers is to produce more advanced composites with much higher mechanical and thermal properties and these products have more opportunity to be used in different industries.

In this study, the influences of addition of HDA on the previously determined rheological and colloidal properties of montmorillonite dispersions were investigated in addition to the reproducibility of rhe-

Correspondence to: N. Güngör (nurfer@itu.edu.tr).
Contract grant sponsor: Istanbul Technical University, Research Fund.

ologic and electrokinetic measurements, XRD, and IR analyses for detail studies. Similar experimental measurements were done to characterize the new composites, which are made by the interaction of OMMT compound with 1% PVA solution.

EXPERIMENTAL

Materials

Natural clay sample was collected from Ünye area east of Black Sea coast of Turkey and they have been identified as mainly smectite group minerals using XRD (Philips PW1140 model X-ray diffractometer) and IR (Jasco model 5300 FT/IR spectrophotometer) analysis techniques.[18] Chemical analyses were performed using a PerkinElmer 3030 model atomic absorption spectrophotometer. The sample had the chemical composition (wt %): SiO_2 70.30; Al_2O_3 15.00; Fe_2O_3 1.10; CaO 1.60; MgO 2.30; Na_2O 1.45; K_2O 1.20; TiO_2 0.30; and LOI 6.45. Hexadecylamine [$CH_3(CH_2)_{15}NH_2$] was purchased from Aldrich Chemical Co. and used as received. $M_w = 241.46$ g/mol. PVA [—$(CH_2CHOH)_n$—] used in this study was purchased from Merck, $M_w = 145{,}000$ g/mol. All other chemicals used in this study were analytical grade.

Preparation of organically modified montmorillonite (OMMT)

MMT powder was dispersed in deionized water at room temperature mixing for 24 h (6 wt % MMT stock dispersion). 20 m*M* HDA stock solution was prepared by dissolving HDA in water which acidified with HCl. Then, 10 mL HDA stock solution and 10 mL 6 wt % MMT stock dispersion mixed together to obtain 4 wt % MMT + 10 m*M* HDA surfactant. Then, these dispersions were shaken for another 24 h at room temperature.

Other dispersions were prepared with the same sample preparation technique, but HDA were added to the 4 wt % montmorillonite in the concentration range of $5 \times 10^{-4} - 10 \times 10^{-3}$ mol/L.

Preparation of PVA/MMT

The same modification procedure prepared for HDA was also applied to PVA. Using the same method, a maximum concentration of 20 m*M* PVA was able to dissolve in water. Consequently, clay + PVA dispersions contain maximum 10 m*M* PVA. Other dispersions were prepared with the same sample preparation technique, but less concentration of PVA was used.

Preparation of organoclay composite (PVA/OMMT)

The same procedures, described earlier for PVA and HAD, are also applied to OMMT. A maximum concentration of 20 m*M* surfactant was able to dissolve in water. Consequently, clay + HDA + PVA dispersions contain maximum 10 m*M* surfactant. Other dispersions were prepared with the same sample preparation technique, but less concentration of PVA was used.

Characterization of the modified montmorillonite

Particle size distribution was measured by using Micrometrics Model 5000D sedigraph, for sample dispersed in water, with calgon and subjected to magnetic mixing. The average particle sizes of sample have been found as 0.50 μm.[18] The specific surface areas of the samples were determined by dye absorption technique. The calculated values of the specific surface are 120 m^2/g.

The flow behavior of the dispersions was measured in a Brookfield DVIII + type low-shear rheometer. The sample was dispersed in water (2% w/w) and shaken for overnight. An adsorption time of 24 h was adopted for the surfactant. The rheological behavior of the clay suspensions was obtained by shear stress (τ)-shear rate γ measurements within 0–350 s^{-1} shear rates. Rheological measurements were carried out in duplicate. Flow curves were analyzed using the Bingham model, where the Bingham yield stress τ is given by the relation

$$\tau = \tau_e + \eta_{pl}\gamma$$

where τ_e is the extrapolated yield value and η_{pl} is the plastic viscosity.

The ζ potential measurements were carried out using a Malvern Instruments, Zetasizer 2000. The optic unit contains a 5mW He—Ne (638 nm) laser. Before the measurements, all the dispersions were centrifuged at 4500 rpm for 30 min. Supernatants were then used for ζ potential measurements. To make an electrophoretic mobility measurement in this instrument, laser beams are crossed at a particular point in the cell. Particles in the cell were illuminated by these beams. At the crossing point of the beams, Young's interference fringes are formed. Particles moving through the fringes under the influence of the applied electric field scatter light whose intensity fluctuates with a frequency that is related to the particle velocity. The photons detected by the photomultiplier are fed to a digital correlator, the resulting function being analyzed to determine the frequency spectrum, from which the mobility and hence the ζ potential are calculated. Measured electrophoretic mobilities were converted to ζ potential using established theories. ζ Potential was measured, injecting a small portion into the cell of the Zetasizer 2000 instrument at room temperature.

Dispersions were dropped onto thin glass slides, and dried at room temperature. The obtained film samples with different HDA concentrations were analyzed by X-ray diffraction (Philips PW 1040). X-ray diffraction (XRD) measurements were performed at room temperature using Ni-filtered and Cu tube. The *d*-spacing of the MMT before and after HDA treatment are calculated using Bragg's relation ($2d \sin\theta = n\lambda$) according to the angle of the (001) diffraction peak in the XRD pattern, where λ (=1.54) corresponds to the wave length of the Cu-Kα radiation used in the diffraction experiment, d to the spacing between diffractional lattice planes, n diffraction order, and θ is the measured half diffraction angle or glancing angle.

FTIR analyses (400–4000 cm^{-1}) were performed on Jasco Model 5300 FTIR spectrophotometer using KBr pellets with a concentration of 0.1%. Spectral outputs were recorded either in absorbance or transmittance mode as a function of wave number.

The morphology of the fractured surfaces of the clay films was investigated with a JEOL JSM-840 scanning electron microscope. SEM measurements were operated at 15 kV. The specimens were frozen under liquid nitrogen, and then fractured, mounted, and coated with gold (300 Å) on Edwards S 150B sputter coater.

RESULTS

Characterization of HDA modified MMT

First, the rheological characterization of the MMT was examined. Rheological parameters are sensitive to solid content. By increasing the solid content of the dispersions, the viscosity and yield value increased. The shear stress and apparent viscosity versus shear rate curves of 1, 2, 3, 4, 5, and 6% w/w of the montmorillonite dispersions have been drawn and the flow models were determined. The shear stress versus shear rate curves for the dispersions containing different concentrations of the MMT samples are shown in Figure 1(a). The dispersions (1, 2, 3, and 4% w/w) of the MMT exhibited Newtonian behavior. The viscosity of a Newtonian dispersion is the ratio of shear stress/shear. The dispersions did not show yield value due to the interaction between the particles in these dispersions is very small. The dispersions (4, 5, and 6% w/w) of the MMT exhibited Bingham plastic behavior and low yield values were measured in these dispersions. The yield value with clay concentration is due to the increase of number of clay particles in the dispersion. The Bingham yield value (extrapolated shear stress) is a criterion of particle–particle interaction and a better parameter for measuring the structure of a flocculated system. The apparent viscosity values at 205 s^{-1} of MMT (5 and 6% w/w) have been found to be 2.25 and 2.70 mPa s, respectively [Fig. 1(b)]. Increasing in more resistance is expected result against to flow regime together with an increase in solid ratio in the system. In the Figure 2(a), the flow curves of 2% w/w bentonite dispersion and the modified clay with 5.91×10^{-4}, 1.87×10^{-3}, 5.61×10^{-3}, and 9.35×10^{-3} mmol/L HDA are displayed, respectively.

It is observed that flow model of 2 wt % clay dispersion did not change until the addition of 5.6×10^{-3} mmol/L HDA. After this addition, the flow type of the dispersion can be defined as Bingham plastic. In Figures 2(b)–2(d) the yield value, apparent viscosity (at two different shear rate) and hysteresis area of montmorillonite dispersions was plotted as a

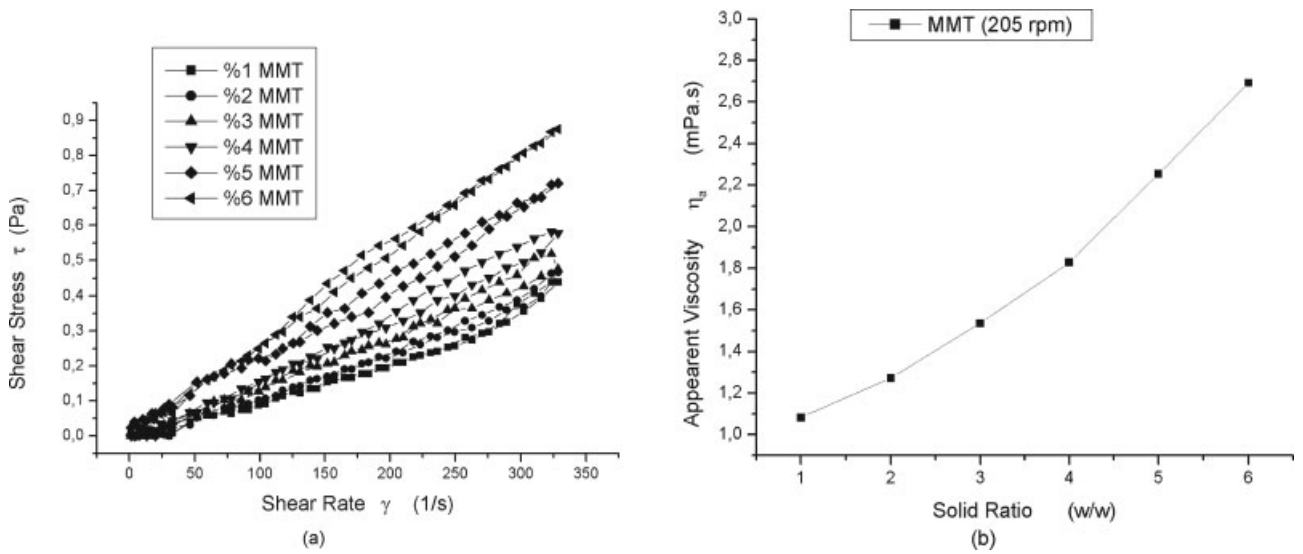

Figure 1 Effect of clay concentration (w/w) on (a) the flow curves and (b) apparent viscosity.

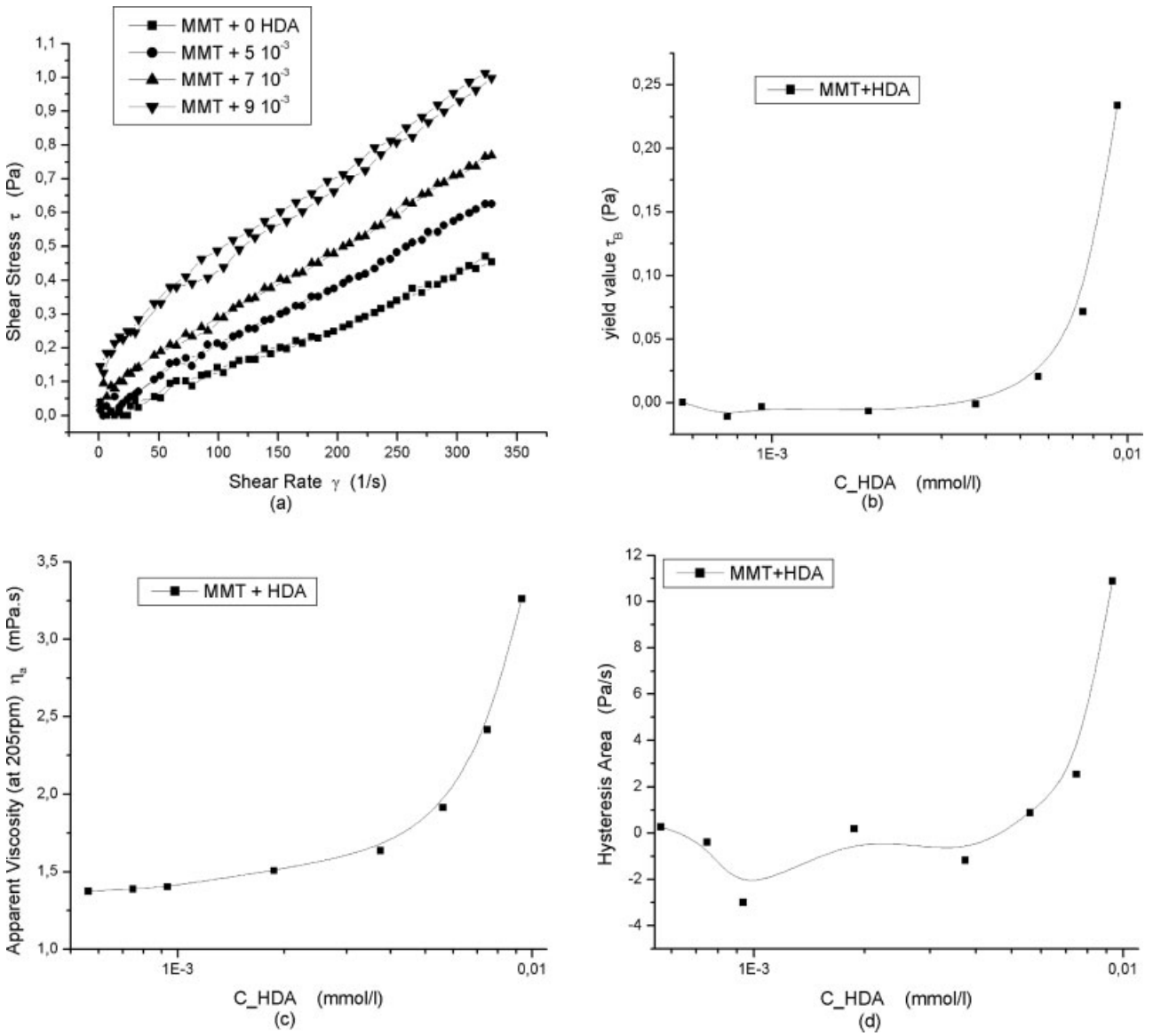

Figure 2 (a) Effect of HDA concentration (w/w) on the flow curves. (b) The changes of the yield value of MMT dispersions with HDA surfactant added to dispersions. (c) The changes of the apparent viscosity (η_a) of MMT dispersions with HDA surfactant added to dispersions. (d) The hysteresis loop area of 2% w/w bentonite dispersion with HDA concentration.

function of increasing HDA concentrations. First addition of surfactant into the bentonite dispersions did not change rheological parameters significantly. As seen from the Figure 2, a significant increase in rheologic parameters is observed after reaching HDA concentration up to 5.6×10^{-3} mmol/L value. This sharp and continuous increase observed in the rheological parameters indicates a gel structure in the dispersion with increasing surfactant concentration. The continuous increase in the rheological parameters is an indicator of a growing network structure in the environment.

Figure 3 shows the change in ζ potential with HDA concentration for MMT dispersions. The ζ potential is an electrical potential in the double layer at the interface between a particle, which moves in an electric field, and surrounding liquid. The surface charge property can be characterized by ζ potential and the stability of a clay solution can be measured depending of its value. HDA show the flocculants effect on the 2% (w/w) clay containing dispersions. However, surfactants are not able to cover up completely clay surfaces. These results are in good agreement with the behavior of rheologic parameters of bentonite dispersion.

The FTIR spectrum of MMT is shown in Figure 4(b) and Table I. The spectrum of MMT shows the characteristic bands 3631 cm^{-1} due to O—H streching (sharp peak), a broad peak centered on 3448 cm^{-1} due to interlayer and intralayer H-bonded O—H,

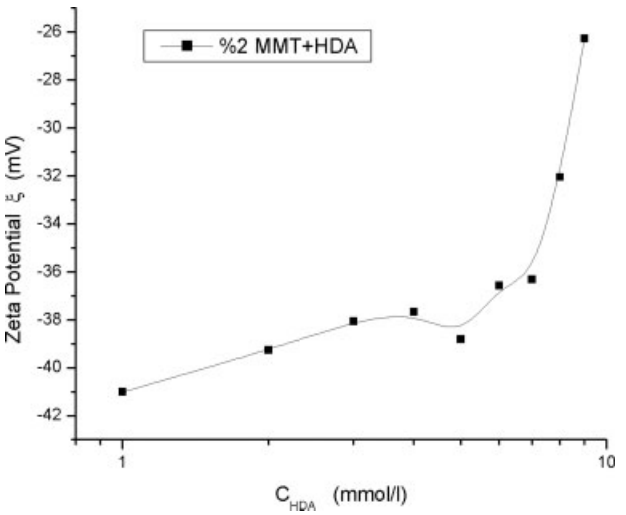

Figure 3 The changes of the zeta potential of MMT dispersions with HDA surfactant added to dispersions.

1640 cm^{-1} due to H—O—H bending, 1035 cm^{-1} with shoulder at 1083 cm^{-1} due to Si—O streching, 916 and 842 cm^{-1} due to Al—O streching and 519 and 467 cm^{-1} due to Si—O—Al modes. The first two bands have comparable intensities.[19] The exchange of simple inorganic cations by the other ions results in the enhancement of the intensity of the 3500–3200 cm^{-1} band along with a reduction of intensities due to Si—O and Al—O. The increase in intensity of the 3500–3200 cm^{-1} band reflects the increased hydrogen bonding between the lattice hydroxyls and organic groups. When the protons in HDA are hydrogen-bonded to the oxygen species of Si—O, Al—O and Si—O—Al segment, Si—O, Al—O and Si—O—Al bonds would be weakened and the tetrahedral symmetry of these moieties will be disttorted. This would result in the change of the IR band positions as well as the reduction of intensities of the bands. It can clearly be seen that the HDA/MMT spectra, exhibit the presence of characteristic absorptions due to the organic and inorganic groups (Table I). Absorbencies due to structural O—H stretching 3626 cm^{-1} and MgAl—OH, Al—O, Si—O bendings at 794, 624, 519, and 467 cm^{-1} confirm the presence of Na-montmorillonite in the dispersion. In the bentonite HDA adsorption products, the O—H stretching peak was broadened and gave a maximum at 3419 cm^{-1}. The hydroxyl stretching frequencies were broadened and bands move to lower frequencies by about 29 cm^{-1}. These shifts may be attributed to formation of hydrogen bonds. The Si—O stretching peak was also broadened and gave a maximum at 1035 cm^{-1} with shoulder at 1087 cm^{-1}. This is attributed to the relaxation of hydrogen bonding between MgAl—OH as well as to the hydrated water of exchangeable cationic metal ions on the montmorillonite surface, further supporting the presence of HDA.

Figure 5 shows the XRD patterns of MMT samples without the organic modification and modified with HDA. X-ray diffraction measurements of surfactants containing films on thin glass micro slide indicated that surfactant molecules were introduced not only on the outer surface, but also within the interlayer spacing. Increasing the amount of surfactant in MMT dispersion enhances the intercalation effect of HDA. The $d_{(001)}$-spacing value is 12.61 Å for MMT dispersion but it expands to 18.40 Å after the addition of 9×10^{-3} mmole/L HDA. This increase in the expansion of basal spacing suggests that intercalated surfactant molecules introduced into the clay galleries. XRD results indicate a bilayer arrangement of the HDA molecules parallel to the silicate layer.[20,21]

Characterization of PVA composites

The mixture of 1 wt % PVA solution, which shows Newtonian flow property, with 0.3 g MMT-clay dispersion displays non-Newtonian flow properties. Experimental studies revealed that the plastic viscosity of PVA/MMT dispersion is 3.13 mPa s and yield value is 0.18 Pa. It interpretated that the changes in the flow model of water-based MMT dispersion, which shows Newtonian flow properties, to Bingham flow model by adding either surfactant or polymer indicates the interaction of additives with clay particles and as a result of this processes, the interactions among clay particles could have been changed. The XRD studies on PVA/MMT dispersions showed that $d_{(001)}$-spacings of MMT-clays expanded 4.4 Å more. This observation indicates that nonionic polymer PVA introduce into the layers of clay particles, like HDA molecules (they have caused the additional expansion of 5.8 Å). The FTIR spectra of PVA/MMT are shown in Figure 4(d). The intensity of the band at 3631 cm^{-1} decreases at 3622 cm^{-1}.

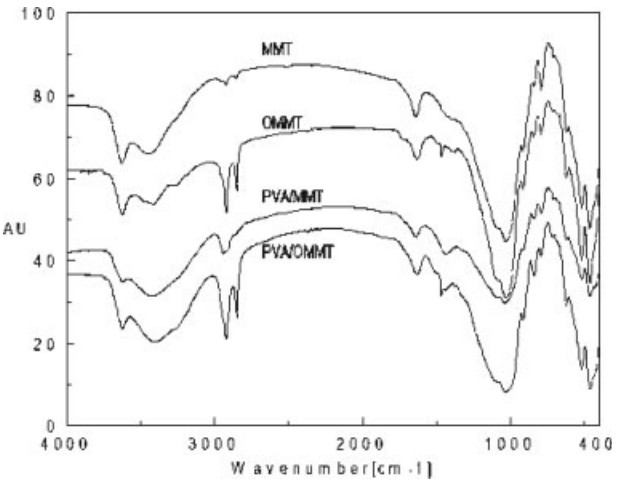

Figure 4 FTIR spectra of MMT, OMMT, PVA/MMT, and PVA/OMMT.

TABLE I
Effects of Hydrogen Bonding on the Hydroxyl and the Other Groups Frequencies

Sample	OH str. (cm^{-1})	Hydrog. vibr. (cm^{-1})	C—H str. and bend. (cm^{-1})	N—H bend. (cm^{-1})	HOH def. (cm^{-1})	Si—O str. (cm^{-1})	Al—O str. (cm^{-1})	Al—O—bend. (cm^{-1})	Si—O bend. (cm^{-1})
MMT	3631	3448	–	–	1640	1035 with 1083	916 and 845	793 and 624	521 and 467
OMMT	3626	3419	2923 and 2851 1469 and 721	1499	1638	1035 with 1087	916 and 845	794 and 624	519 and 467
PVA/MMT	3622	3414	2944, 2916, 2863, 1437, 1384	–	1640	1038 with 1087	916 and 842	793 and 627	519 and 467
PVA/OMMT	3626	3401	2923, 2851, 1469, 1441, 1380 and 721	1508	1638	1035 with 1081	915 and 843	796 and 626	519 and 463

The intensity of the band in the range 3448 cm^{-1} is found to 3414 cm^{-1}. The hydroxyl stretching frequencies were broadened and bands move to lower frequencies by about 34 cm^{-1}. The intensities of the Si—O and Al—O bands are also changed (Table I). This suggests that the newly formed polymer continues to be in a position to interact with Si—O and Al—O bonds. This observation is in agreement with our explanation of the change in $d_{(001)}$-spacings observed in the XRD studies.

1 wt % PVA solution shows Newtonian flow properties. The rheological characterization of PVA/OMMT dispersion, which was obtained by the treatment of 1 wt % PVA and 0.3 g HDA solutions, was determined. Apparent viscosity is 3.24 mPa s at 205 rpm, histeresis area is 0.80, dispersion displays Newtonian flow and no yield value is observed. Figure 6 shows the flow curves of MMT, OMMT, PVA/MMT, and PVA/OMMT systems. The determination of yield values of OMMT and PVA/MMT dispersions suggest that the components of these dispersions interact with each other more closely, and consequently,

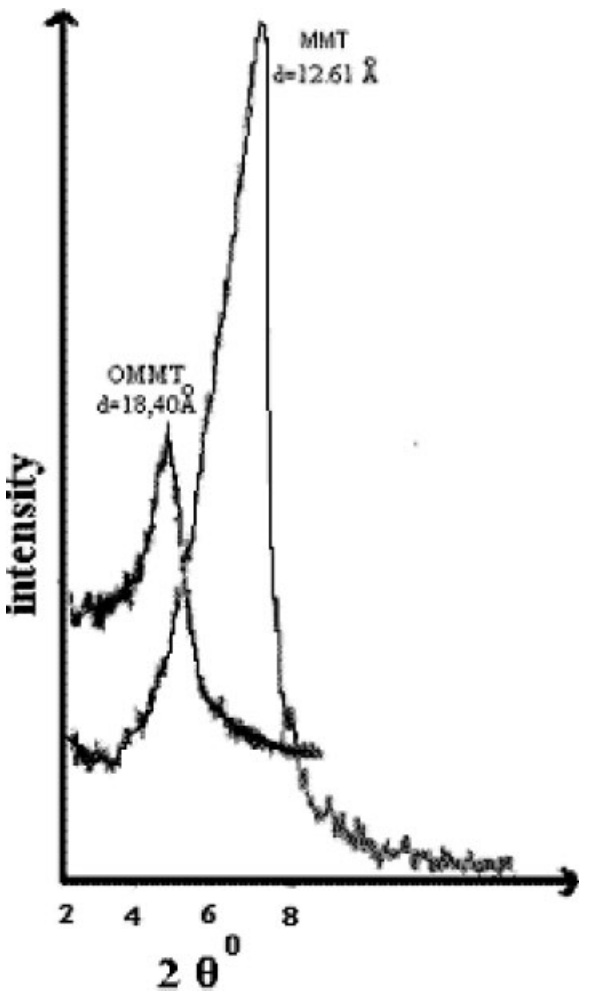

Figure 5 XRD patterns of MMT and OMMT composites.

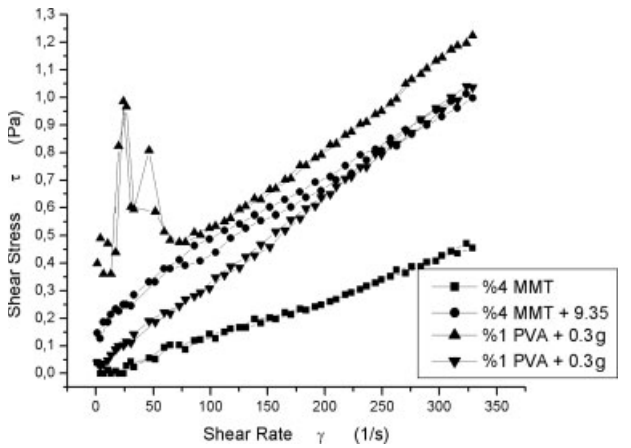

Figure 6 The flow curves of MMT, OMMT, PVA/MMT, and PVA/OMMT dispersions.

more gel structure is formed. No yield value is obtained in water-based PVA/OMMT system, which is made by the interaction of OMMT organoclay and PVA polymer. This observation suggests that some current clusters in OMMT dispersed after the adding of PVA solution.

The $d_{(001)}$-spacings are measured about 15.5 Å in PVA/OMMT composites in XRD studies. The XRD measurements of organoclays are listed in Table II. The main question is that why *d*-spacings swell to 18.4 Å after OMMT and decrease to 15.5 Å after PVA/OMMT treatments? This shift from 18.4 to 15.5 Å in the *d*-spacings of OMMT layers is caused by dehydration within clay layers. It is possible to suggest that H-bonds formed between organic molecules and clay layers. Consequently, this solvent removal process causes a reduction in *d*-spacings between the clay layers. This also implies that a large amount of organoclay cannot be exfoliated in PVA/OMMT; it exists in the form of an intercalated layer structure as a result of dehydration to PVA.[13,14] By this way, organic molecules caused squeezing of the clay layers, which indicate the presence of ''unit cell scale'' aggregation configuration of OMMT that are familiar in the case of high clay loading for the nanocomposites.

The spectrum of PVA/OMMT in Figure 4(a) also contains characteristic absorbance bands of all components (Table I). The peak corresponding to structural hydroxyl stretching at 3626 cm^{-1} was attributed to montmorillonite. The broad peak centered on 3401 cm^{-1} was assigned to O—H stretch. HOH deformation peak centered at 1638 cm^{-1} was also present in the FTIR spectrum. The absorption bands at 1035 with shoulder at 1081, 796, 626, 519, and 463 cm^{-1} belong to Si—O—Si, MgAl—OH, Al—O, Si—O—Mg, and Si—O—Fe vibrations, respectively. The hydroxyl stretching frequencies were broadened and bands move to lower frequencies by about 47 cm^{-1}. These shifts may be attributed to formation of hydrogen bonds. The intensities of the band in the range 3600 cm^{-1} decrease in the order of MMT < OMMT ≈ PVA/OMMT < PVA/MMT. In the intensities of the band in the range 3500–3200 cm^{-1}, on the other hand, is found to decrease in the order MMT < OMMT < PVA/MMT < PVA/OMMT. The intensities of the Al—O stretching bands decrease and Al—O bending bands increase in the order MMT ≈ OMMT < PVA/MMT < PVA/OMMT. Absorbtion bands of Al—O vibration for PVA/MMT and PVA/OMMT are different than those for the MMT (Table I). This is attributed to the relaxation of hydrogen bonding between (Al—O) O—H bending as well as to the hydrated water of exchangeable cationic metal ions on the montmorillonite surface. This observation is in agreement with our explanation of the change in $d_{(001)}$-spacings observed in the XRD studies. The ζ potential of PVA/OMMT dispersion is measured as 2.3 mV. In contrast, ζ potential of MMT dispersion was measured as −41 mV and OMMT dispersion was −26.25 mV (Fig. 3). Like data obtained from FTIR and XRD analyses, positive values of ζ potential indicate that PVA molecules attached on the surface of organoclay particules. These ζ potential data is another method to show these attachments of PVA molecules on organoclay particles.

Scanning electron microscopy (SEM) micrographs of the samples were used for characterization of the montmorillonite dispersions with HDA, PVA, and PVA/HDA (Fig. 7). All flake structures in 2 wt % clay dispersion display severe undulated surfaces without clear flake structure in SEM studies [Fig. 7(a)]. When HDA (9×10^{-3} mmol/L) were added, not homogeneous morphology became apparent, and therefore, we expect more expansion between crystal layers [Fig. 7(b)]. The unmodified montmorrillonite shows aggregates and layer structures, voids and some deformed portions may result from the coarseness of the fractured surface [Fig. 7(a)]. Besides, Figure 7(b) displays more aggregate flaky texture in HDA/MMT samples, of which are not homogenous. This is probably related to consequence of the agglomeration of some clay particles. Conversely, from the fractured surface of PVA/MMT and HDA/PVA/MMT composites [Figs. 7(c) and 7(d)] are shown not only the smooth surface due to finely dispersed MMT particles but also, no trace of MMT particles. This is probably the consequence of the regular dispersion of micron-sized MMT particles. The stack sizes of PVA/MMT and

TABLE II
XRD Results of Samples

Sample	XRD peak position (2°θ)	$XRD_{d(001)}$ (Å)
MMT	7	12.61
OMMT	4.8	18.39
PVA/MMT	5.2	16.97
PVA/OMMT	5.7	15.49

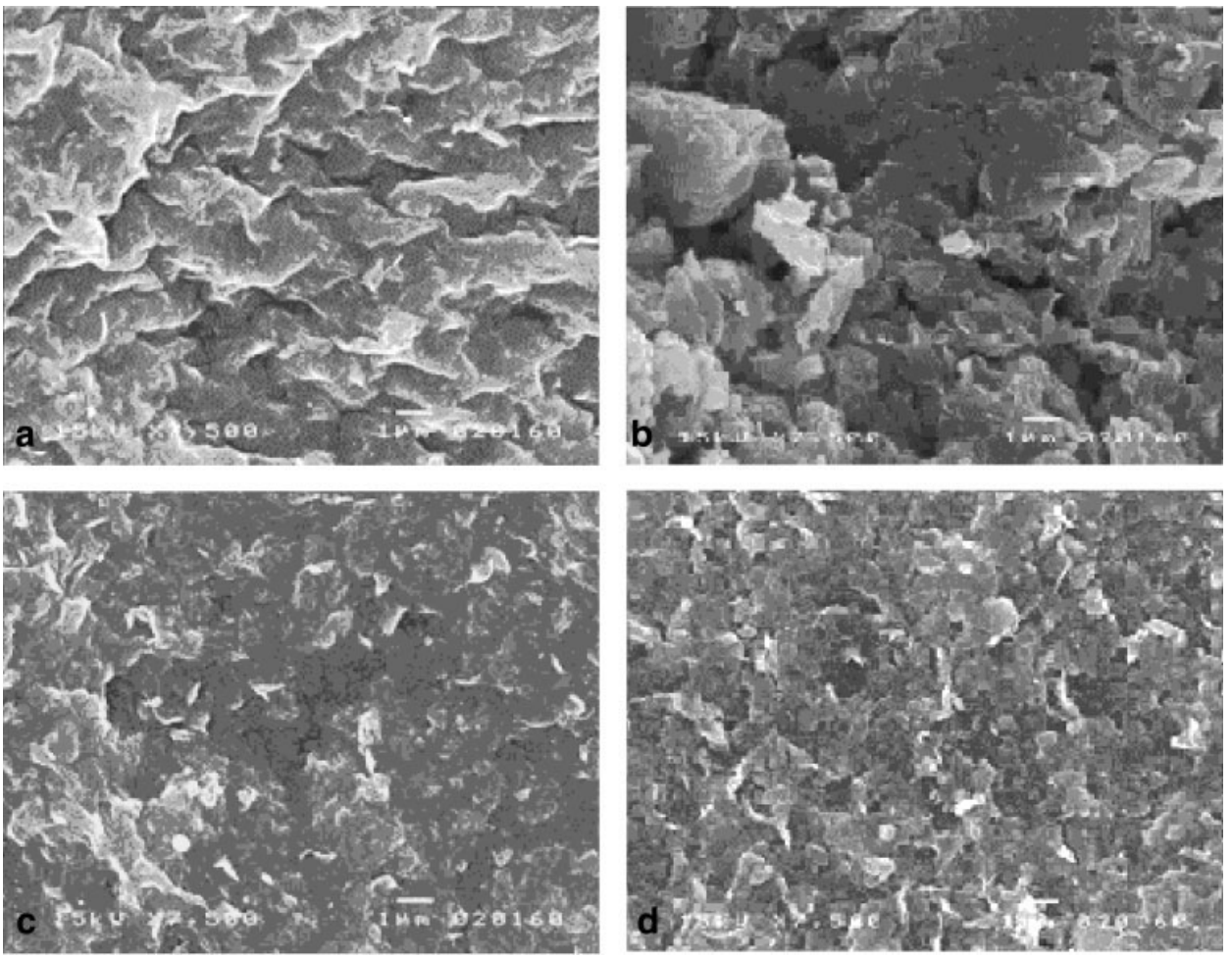

Figure 7 SEM microphotographs of (a) MMT, (b) OMMT organoclay, (c) PVA/MMT, and (d) PVA/OMMT.

PVA/OMMT found from the particle sizes are about 1–1.5 μm and 0.6–1 μm, respectively.

CONCLUSIONS

The adsorbed HDA affects the rheological and electrokinetic properties of MMT dispersions. The degree of interaction between HDA and the bentonite particles depends on the HDA concentration in the suspension. Addition of the HDA and PVA in 2% w/w of clay dispersion created a flocculent effect. The ζ potential measurements have been displayed that the HDA molecules hold on the clay particle surfaces and the XRD analyses have been displayed that they get into the basal intervals. XRD results indicate a bilayer arrangement of the HDA molecules parallel to the silicate layer. The FTIR spectra can clearly be seen that all spectra exhibit the presence of characteristic absorptions due to the organic and inorganic groups. FTIR results show that the HDA and PVA molecules and clay particles interact with each other and, OMMT interacts more into the layers of montmorillonites, but PVA/MMT and especially PVA/OMMT interacts more near the surface of montmorillonites.

The authors thank to Assist. Prof. Gültekin Göller providing SEM studies in his laboratory.

References

1. Lagaly, G. Appl Clay Sci 1998, 4, 105.
2. Angle, C. W.; Hamza, H. A. Appl Clay Sci 1989, 4, 263.
3. Alemdar, A.; Güngör, N.; Ece, Ö. I.; Atıcıı, O. J Mater Sci 2005, 40, 171.
4. Permien, T.; Lagaly, G. Clay Miner 1994, 29, 751.
5. Tombacz, E.; Szekeres, M.; Baranyi, L.; Micheli, E. Colloids Surf A: Physicochem Eng Aspects 1998, 141, 379.
6. Luckham, P. F.; Rossi, S. Adv Colloid Interface Sci 1999, 82, 43.
7. İşçi, S.; Ece, Ö. I.; Güngör, N. J Compos Mater 2006, 40, 1105.
8. Pinnavaia, T. J.; Beall, G. W., Eds. Polymer-Clay Nanocomposites, Wiley: New York, 2000.
9. İşçi, S.; Günister, E.; Ece, Ö. I.; Güngör, N. Mater Lett 2004, 8, 1975.
10. Strawhecker, K. E.; Manias, E. Chem Mater 2000, 12, 2943.
11. Lee, D. C.; Lee, W. J. J Appl Polym Sci 1996, 61, 1117.
12. Sheng, G.; Xu, S.; Boyd, S. A. Water Res 1996, 30, 1483.

13. Chang, J. H.; Park, D. K.; Ihn, K. J. J Polym Sci, Part B: Polym Phys 2001, 39, 471.
14. Chang, J. H.; An, Y. U. J Polym Sci Part B 2002, 40, 670.
15. Chang, J. H.; Park, D. K.; Ihn, K. J. J Appl Polym Sci 2002, 84, 2294.
16. Chang, J. H.; An, Y. U.; Sur, G. S. J Polym Sci, Part B: Polym Phys 2003, 41, 94.
17. Chen, C.; Curliss, D. Nanotechnology 2003, 14, 643.
18. Yalçın, T.; Alemdar, A.; Ece, Ö. I.; Güngör, N. Mater Lett 2002, 57, 420.
19. Marel, H. W.; Beutelspacher, H. Atlas of Infrared Spectroscopy of Clay Minerals and Their Mixtures; Elsevier: Amsterdam, 1976.
20. Boyd, S. A.; Jaynes, W. F. InLayer Charge Characteristics of 2:1 Silicate Clay Minerals; Mermut, A. R., Ed.; The Clay Minerals Society: Boulder, CO, 1994; vol. 6, p 48.
21. Laird, D. A. In Layer Charge Characteristics of 2:1 Silicate Clay Minerals; Mermut, A. R., Ed.; The Clay Minerals Society: Boulder, CO, 1994; vol. 6, p 80.